Marco Cavaliere[ab]*, Conor Walsh[a], Herman Alexander Jaeger[ab], Kilian O'Donoghue[b], Pádraig Cantillon-Murphy[ab]

[a]University College Cork, Cork, Ireland;
[b]Tyndall National Institute, Cork, Ireland

*Corresponding author: m.cavaliere.ucc@gmail.com

Marco Cavaliere (Member, IEEE) received the Laurea degree in energy engineering and the Laurea Magistrale degree in electrical energy engineering from the University of Padua, Italy, in 2017 and 2019, respectively. He is currently pursuing a Ph.D. degree in electrical and electronic engineering with the University College Cork and the Tyndall National Institute, Cork, Ireland. His current research interests include electromagnetic tracking and navigation systems for image-guided interventions.

Conor Walsh received the MEng degree in Electrical & Electronic Engineering from University College Cork, Ireland, in 2021. He is currently working as a Graduate R&D Electrical Engineer in the medical device industry.

Herman Alexander Jaeger (Member, IEEE) received the B.E., M.Eng.Sc., and Ph.D. degrees in electrical and electronic engineering from University College Cork (UCC), Ireland, in 2014, 2015, and 2018, respectively. He is currently a Postdoctoral Researcher with UCC. His current research interests include electromagnetic tracking and navigation for image-guided interventions.

Kilian O'Donoghue received the B.E. and Ph.D. degrees in electrical and electronic engineering from University College Cork, Ireland, in 2011 and 2015, respectively. His research interests include EM tracking systems, circuit design, magnetic field modelling, and minimally invasive surgeries.

Pádraig Cantillon-Murphy received the B.E. degree from UCC in 2003, and the M.Eng.Sc. and Ph.D. degrees from the Department of Electrical Engineering and Computer Science, Massachusetts Institute of Technology (MIT), in 2005 and 2008, respectively. He is currently a Senior Lecturer of electrical and electronic engineering with University College Cork, Ireland, an Academic Member of the Tyndall National Institute, and an Honorary Faculty with L'Institutde Chirurgie Guidée par l'Image, Strasbourg. He is also a Principal Investigator with the Biomedical Design Laboratory, UCC, and the Tyndall National Institute which explores novel device development in image-guided surgery and endoscopy. His current research interests include magnets for surgery, electromagnetic tracking and navigation, and surgical robotics.

Magnetic tracking using a modular C++ environment for image-guided interventions.

Magnetic tracking enables instrument tracking for image-guided interventions when no line of sight is available. This paper describes the first steps towards a more cost-effective, modular, and adaptable approach that builds upon prior work in open hardware architectures for magnetic tracking in image-guided interventions. An exemplary C++ framework is implemented and demonstrated with the open-hardware Anser EMT system. System performance in speed, accuracy, and precision of the C++ implementation is analysed. Static positioning accuracy and precision are calculated within the Region of Interest (ROI) and an average position error of 1.0 ± 0.1 mm is demonstrated. Results show an indicative increase in the update rate using the C++ framework and substantially lower memory requirements, compared to the previously optimised Python and Matlab solvers. These preliminary results provide the basis for future development which will integrate the C++ framework in a 3D Slicer module, greatly extending the adaptability of the platform for customization in advanced image-guided procedures.

Keywords: Magnetic Tracking; C++ framework; Open-source

1 Introduction

Magnetic tracking, or electromagnetic tracking (EMT), enables instrument tracking and navigation during image-guided interventions with no line of sight limitation (Peters and Cleary 2008; Cleary and Peters 2010). EMT is used during clinical diagnosis or therapy using flexible bronchoscopy and in orthopaedic procedures (Franz et al. 2014; Herman Alexander Jaeger et al. 2019). The technology finds also application in robotic surgical devices for guidance and navigation in the absence of a line of sight (Schwein et al. 2017; 2018), as well as in Virtual and Augmented Reality in surgery (Halabi et al. 2020). Magnetic tracking can also be used in multi-modal imaging applications combining traditional radiological imaging such as CT, with ultrasound and other local imaging modalities (Franz et al. 2019), for example for percutaneous hepatic intervention (Lee 2014, 20; Akhtar et al. 2021).

Several commercial magnetic tracking systems are available which are based on the OEM Aurora system (‘Electromagnetic Measurement Systems’ n.d.) from NDI (Northern Digital Inc., Waterloo, Canada). For example, SCOPEPILOT (PENTAX Medical, Hamburg, Germany) provides intuitive navigation in colonoscopy, MediGuide Technology (Abbott Laboratories, Chicago, IL, USA) facilitates cardiovascular procedures in the electrophysiology (EP) lab, the SPiN Thoracic Navigation System (Veran Medical Technologies, St. Louis, MO, USA) is used in image-guided bronchoscopy, and the Monarch Platform (Auris Health Inc., Redwood City, CA, USA)

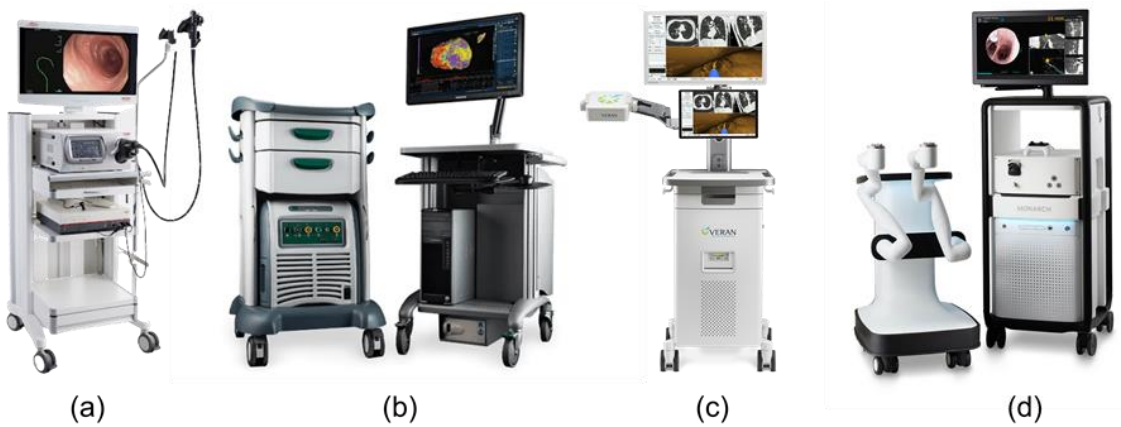

Figure 1. Examples of clinical applications for magnetic tracking technology: (a) Pentax ScopePilot, colonoscopy; (b) Abbott MediGuide, EP navigation; (c) Veran SPiN, thoracic navigation; (d) Auris Monarch, robotic bronchoscopy.

enables robotic endoscopy. Pictures of these systems are shown in Figure 1.

Other commercial magnetic tracking systems are: ScopeGuide (Olympus Corporation, Shinjuku, Tokyo, Japan) for colonoscopy and enteroscopy, the CARTO 3 System (Biosense Webster, Irvine, CA, USA) for EP mapping and navigation, and the superDimension Navigation System (Medtronic, Minneapolis, MN, USA) for airway navigation.

However, the *black-box* nature of these systems has led to the development of the open-hardware Anser EMT project (‘Anser EMT | Open Science Framework’ n.d.), which offers an open hardware architecture (Mansfield et al. 2014) using both Matlab (Natick, Massachusetts: The MathWorks Inc.) and Python (Van Rossum and Drake 2009) frameworks for development (Herman Alexander Jaeger et al. 2017; Herman Alexander Jaeger, Hinds, and Cantillon-Murphy 2018).

The platform has enabled subsequent hardware innovation with bespoke sensor design (Franz et al. 2019; Cavaliere et al. 2020), custom tracking volumes (H. A. Jaeger and Cantillon-Murphy 2019) as well providing a basis for characterising and compensating for magnetic distortions (Herman Alexander Jaeger and Cantillon-Murphy 2018; H. A. Jaeger and Cantillon-Murphy 2019; Cavaliere et al. 2021).

The Anser EMT software framework and solver algorithm have previously been implemented in Matlab and Python, the shortcomings of which are apparent. Matlab requires a license to use and has poor hardware support for operating systems outside of Microsoft Windows. Python is free and well supported by open-source libraries, but considerable time and memory overhead are required for either implementation.

This article describes the preliminary performance of a C++ framework and solver implementation using the Anser EMT system. This is an important step in the effort to develop open-source platforms for navigated image-guided interventions (Ungi, Lasso, and Fichtinger 2016). The paper presents a full, application-independent,

open-hardware EMT system that can potentially integrate with existing hardware and software in any operating environment.

1.1 Background to the Modular Anser EMT Framework

As previously described in detail (Herman Alexander Jaeger, Hinds, and Cantillon-Murphy 2018), the software system of an electromagnetic tracking system such as Anser can be described as having four main components:

- **Acquisition:** The first step in solving for sensor position and orientation is to acquire the signal from a magnetic tracking coil. The coil experiences an induced voltage from a set of 8 sinusoidal magnetic sources, which is sampled using a USB-6216 acquisition device (National Instruments, Austin TX, USA).

- **Filtering:** The sampled signal is digitally filtered to extract the magnetic flux due to each magnetic source. It can be shown that at least five or more different sources are required to reach a well-defined position and orientation solution for a single-axis (5DOF) tracking coil (Plotkin et al. 2010).

- **Modelling:** A physical model of the interaction between the magnetic sources and tracking coil is calculated in software from the Bio-Savart law (Haus and Melcher 1989; Sonntag et al. 2007). Variations on this approach using mutual inductance models and magnetic dipole approximations have also been used in other systems (Bien et al. 2014; De Angelis et al. 2017; Cavaliere et al. 2021).

- **Solving:** The difference between the filtered measurements from the tracking coil and physical model form an objective function, shown in Equation (1,

$$\mathrm{F}(\mathrm{x},\mathrm{y},\mathrm{z},\theta,\varphi) = \sum_{\mathrm{i}=1}^{8}\left(\Phi^{\mathrm{i}}_{\mathrm{meas}} - \Phi^{\mathrm{i}}_{\mathrm{calc}}\right)^2 \qquad (1)$$

  where Φ^{i}_{meas} and Φ^{i}_{calc} are the measured and modelled magnetic fluxes respectively, and $(\mathrm{x},\mathrm{y},\mathrm{z},\theta,\varphi)$ is the position and orientation of the tracking coil in spherical coordinates. Equation (1) is minimised using the Levenberg–Marquardt algorithm (Levenberg 1944), which was demonstrated to be optimal for this application (Shafrir, Paperno, and Plotkin 2010).

The position and orientation solver can be integrated with the tracking system hardware, other operating room equipment and with a host PC, as shown in Figure 2. The *OpenIGTLink* API (Tokuda et al. 2009) was used in conjunction with 3D Slicer (Kikinis, Pieper, and Vosburgh 2014) for demonstration purposes. The modular approach allows for integration with other navigation platforms, *e.g.* CustuX (Askeland et al. 2016) or MITK (Wolf et al., n.d.).

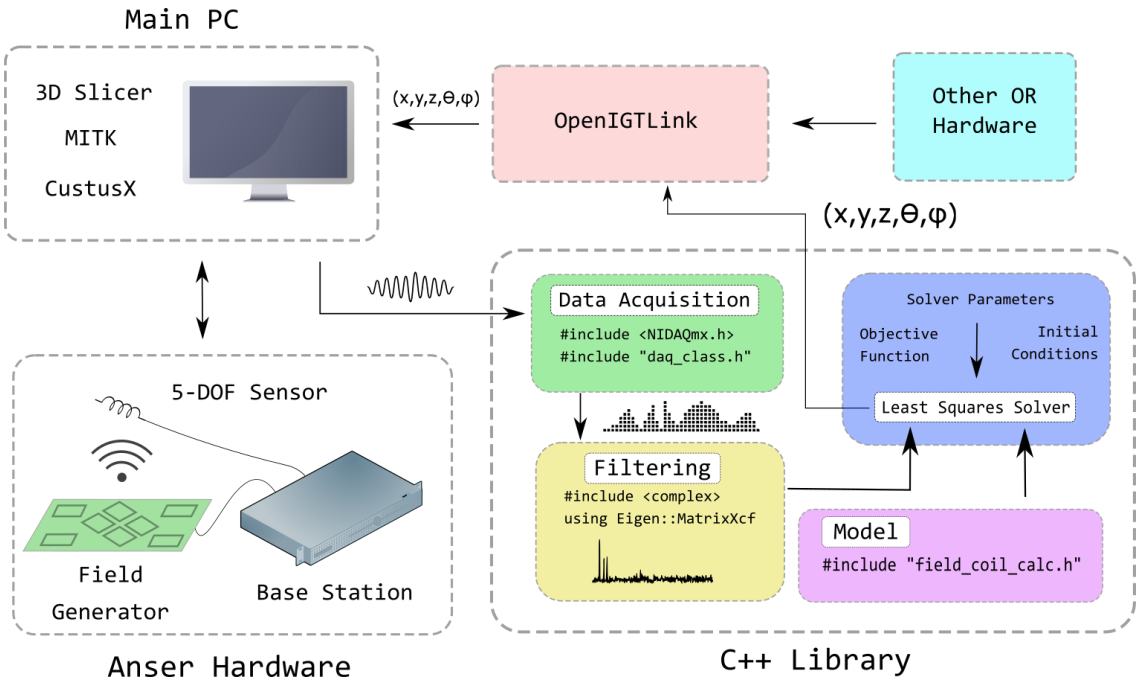

Figure 2. A schematic representation of the overall data flow in the Anser EMT system. The solver module of the C++ library is the focus of the work in this paper.

Previous work has shown the feasibility of using this approach to develop an open framework enabling magnetic tracking using Python. In this work, the approach is extended to create a modular open-source C++ environment.

2 Material and Methods

2.1 Anser .cpp Library Implementation

A library was created to package all of the source code into corresponding classes for each stage presented in Section 1.1, as shown in Figure 2. Linear algebra functionality in C++ was enabled by the Eigen3 library (Guennebaud and Jacob 2010).

To test the C++ implementation of the solving stage, a .cpp test-file was created which implements the solver class, as described in Figure 3.

The file imports a .csv file of the previously recorded sensor measurements and extracts them into a matrix Figure 3(a). A simple instance of the class is declared Figure 3(b) and the initial conditions are set Figure 3(c). The main setup functions are called Figure 3(d) which model the magnetic fields, specify the solving parameters and set the calibration vector within the cost function. Each row vector is then passed to the solving method along with the initial conditions. The resulting solution is finally saved to an output file Figure 3(e).

An identical approach was used for Matlab and Python implementations, allowing the three solvers to be objectively compared.

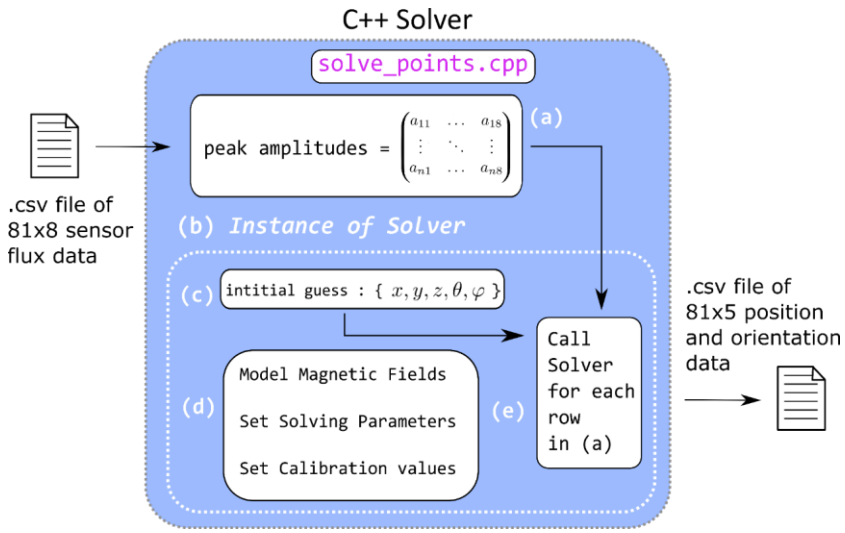

Figure 3. A basic overview of a .cpp file that implements the solver library to solve the recorded values from the experiment.

2.2 Experimental setup

A commercial 5DOF sensor (model *610158*, Northern Digital Inc., Waterloo, Canada) was placed at 81 different locations above the Anser EMT field generator, in a 9×9 horizontal grid, and the corresponding sensor flux was measured and recorded. The experiment was repeated for two different sensor orientations, along axes Y and Z defined in Figure 4, and two different heights, at 10 cm and 20 cm from the planar transmitter board.

A 2D linear actuator was used to move the sensors repeatedly and consistently. The robot was mounted on a wooden frame, to keep it at more than 1 m from the Region of Interest (ROI) and avoid magnetic field interference. The precise sensor position and orientation at every test point was measured by the Polaris Vega optical system (Northern Digital Inc., Waterloo, Canada). Two magnetic sensors were attached to a 3D printed optical tool, *APPLE01* from the open-source library (Brown et al. 2018), for a fast sampling of orthogonal directions. The full experimental setup is shown in Figure 5.

The sampling and demodulation stages were implemented using Matlab to isolate the performance comparison of the three solver implementations, in Matlab, Python, and C++. For a given sampling frequency and duration, there is no difference in the sampling stage for different languages, since they all use the same background Windows driver (NI-DAQmx). The demodulation time is in the order of µs and has little or no impact on the overall speed and accuracy performance of the system, as the majority of computation is done in the final solving stage.

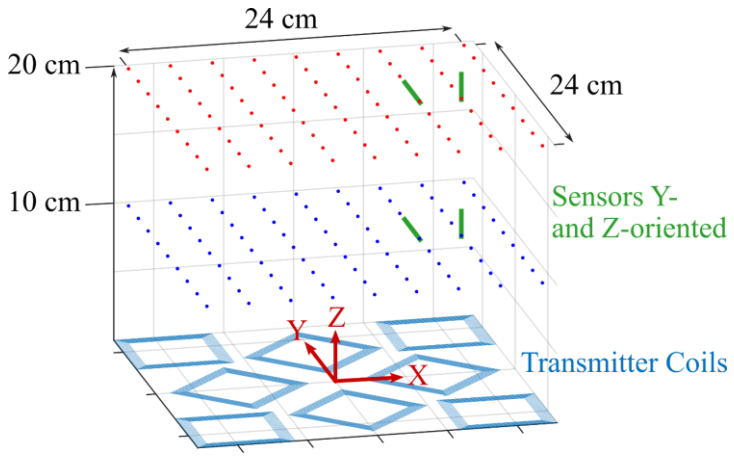

Figure 4. The magnetic field generated by the 8 transmitter coils was measured at two grids of 81 points, for two sensor orientations.

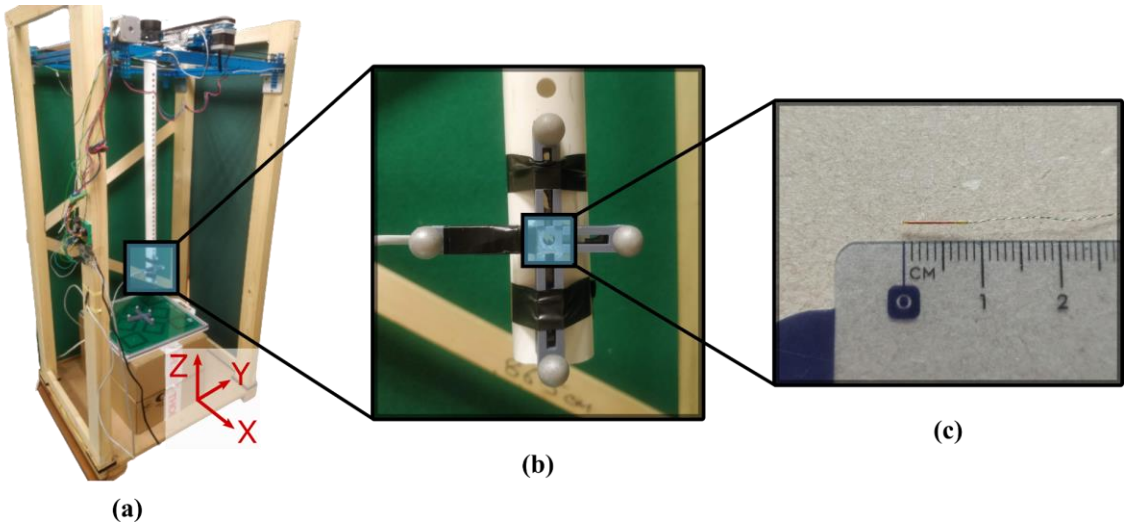

Figure 5. Experimental setup. (a) The XY robot moves the magnetic sensor on a plane. A wooden frame is used to keep metallic components at 1 m from the ROI, to avoid magnetic field distortions. (b) Two inductive sensors are mounted on an optical tool for ground-truth position reference. The tool is fixed to a PCL pipe. (c) Enlargement of the magnetic sensor.

2.3 Accuracy and precision evaluation

At each test-point, 50 field measurements were collected and the solver used Equation (1) to find the sensor position and orientation. The average solution was considered as tracked sensor position at every test-point, $\overline{p}_i$.

The position accuracy was defined as the Euclidean distance between the tracked and the real position, p^*. The absolute error Δr_i of a single position, i, is given by Equation (2):

$$\Delta r_i = \|\overline{p}_i - p_i^*\| = \sqrt{\Delta x_i^2 + \Delta y_i^2 + \Delta z_i^2} \quad (2)$$

where Δx_i, Δy_i and Δz_i are the Cartesian errors at that position.

The absolute error was calculated for every test-point and the average was taken to determine the global accuracy, or *mean absolute error*, as given by Equation (3):

$$\bar{r} = \frac{1}{P}\sum_{i=1}^{P} \Delta r_i \tag{3}$$

where P is the total number of points.

Another statistical measure of the global accuracy is the 95% Confidence Interval (CI). With a total number of 81 test-points, the 95% CI was determined by the first 77 test-points, sorted by the smaller Euclidean error. In other words, there are 4 test-points which resulted with a positional error larger than the 95% CI reported.

The standard deviation of the fifty solutions at each test-point was calculated for the three coordinates X, Y, and Z, and summed in quadrature as a measure of the system spatial precision at that test-point, σ_i. The root-mean-square was taken to determine the global precision, as given by Equation (4):

$$\bar{\sigma} = \sqrt{\frac{1}{P}\sum_{i=1}^{P} \sigma_i^2} = \sqrt{\frac{1}{P}\sum_{i=1}^{P} \sigma_{Xi}^2 + \sigma_{Yi}^2 + \sigma_{Zi}^2} = \sqrt{\bar{\sigma}_X^2 + \bar{\sigma}_Y^2 + \bar{\sigma}_Z^2} \tag{4}$$

where $\overline{\sigma_X}$, $\overline{\sigma_Y}$, and $\overline{\sigma_Z}$ are the root-mean-square of the standard deviations along the X, Y, and Z coordinates respectively.

2.4 Measuring Time and Memory Requirements

Solver time is a critical parameter for magnetic tracking systems, because it directly reflects on the update-rate and latency of the system, which are important for a smooth, real-time navigation. Timing values for each solver implementation were determined by looping the solving section of the code fifty times and recording the average time to solve a given grid of points. This gave a better estimate of mean solving times and update-rates.

Memory usage was determined using the *memory* function in Matlab which returns the total amount of RAM required to run the given .m file. Unlike Python and C++, the whole instance of Matlab is required for operation and so this is the minimum amount of memory necessary for this operation. The *psutil* library was imported when determining memory usage in Python. This library can retrieve information on running processes and system utilization. Visual Studio natively provides memory usage when a process is running.

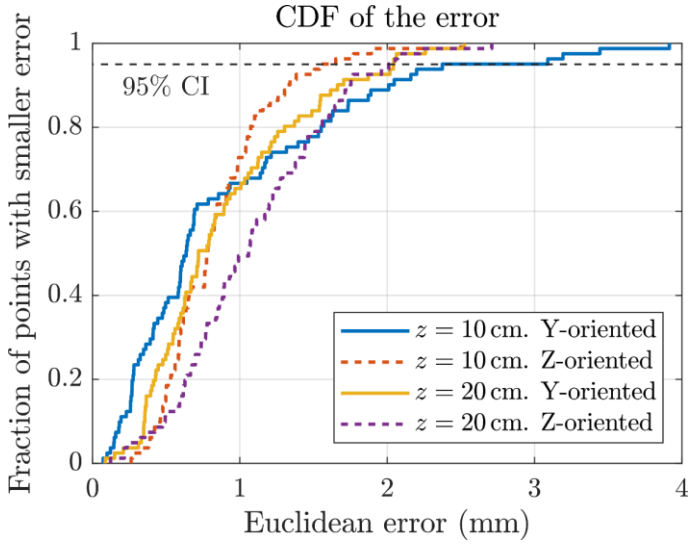

Figure 6. Cumulative Distribution Function of the Euclidean position error calculated at test-points as per Equation (2).

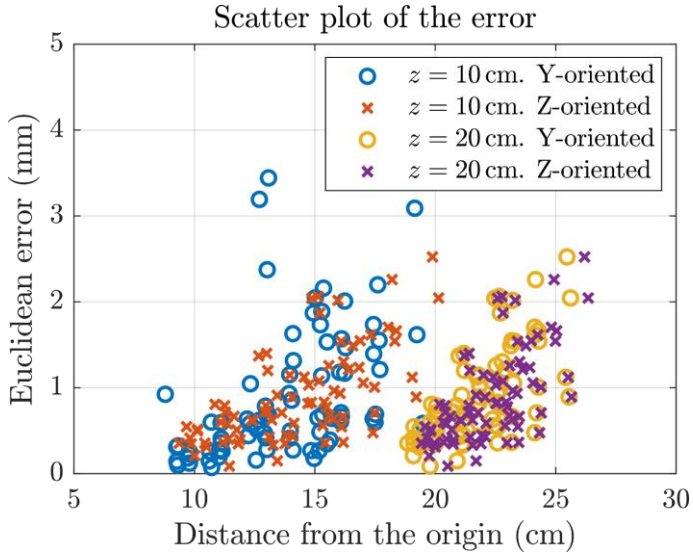

Figure 7. Scatter plot of the Euclidean position error versus the distance of the test-point from the field generator centre.

3 Results

The C++ position error results are plotted in Figure 6 and Figure 7, for the four static tracking experiments. Figure 6 shows the Cumulative Distribution Function (CDF) of the Euclidean error at each test-point, while Figure 7 displays how this error is correlated to the distance from the field generator centre.

The global accuracy and precision calculated from Equations (3) and (4) are reported in Table 1. Similar results were recorded for the Python and Matlab solvers outputs, although these are not included for the sake of brevity.

Table 1. Accuracy and precision measurements for four experiments, computed as per Equations (3) and (4). All values are in millimeters.
[1] with Tabletop Field Generator.
[2] with Flat Field Generator.

Test	$\bar{r}$	**95% CI**	$\bar{\sigma}$	$\overline{\sigma_X}$	$\overline{\sigma_Y}$	$\overline{\sigma_Z}$
z=10 cm. Y-oriented	0.93	2.37	0.10	0.06	0.05	0.07
z=10 cm. Z-oriented	0.84	1.54	0.07	0.05	0.04	0.02
z=20 cm. Y-oriented	0.90	2.04	0.17	0.10	0.10	0.09
z=20 cm. Z-oriented	1.09	2.01	0.22	0.15	0.15	0.03
NDI Aurora[1]	1.20	1.80	N/A	N/A	N/A	N/A
3D Guidance[2]	1.02	2.33	0.61	N/A	N/A	N/A

Table 2. Solver performance for each programming environment. The entire grid of points was solved 50 times and the average result was taken for the results shown.

	Matlab	**Python**	**C++**	**NDI Aurora**	**3D Guidance**
Solving time [ms]	25.9	32.8	18.4	N/A	N/A
Memory usage [MB]	1473	97	1.2	N/A	N/A
Update rate [Hz]	38	31	54	40	80

A thorough comparison of the main optical and magnetic tracking systems available on the market can be found in (Sorriento et al. 2020). Between all, the NDI Aurora with Tabletop Field Generator and the Ascension 3D Guidance (Ascension Technology Corp., Milton, VT, USA) with Flat Field Generator are the systems more close to the Anser EMT system studied in this work, because they all operate with a planar magnetic field generator. For convenience, the position errors of NDI Aurora and Ascension 3D Guidance are reported in Table 1 (Wilson et al. 2008).

The speed of each solver and their corresponding memory requirements were recorded as described in Section 2.4, and are summarised in Table 2. The values are obtained for a laptop PC mounting an Intel i5-6200u CPU, 8 GB RAM and Windows 10 OS. Matlab 2017b, Python 3 in VS Code and the Visual C++ compiler in Visual Studio 2019 were used in this comparison. Update-rates of NDI Aurora and Ascension 3D Guidance are also reported in Table 2.

4 Discussion

The results of Table 1 demonstrate that the system can achieve sub-millimetre accuracy with high repeatability, in a tracking volume of $24 \times 24 \times 24$ cm. As expected, Figure 7 shows that points in the centre of the ROI can be solved with higher accuracy.

It should be noted that, while the positioning error of the Anser EMT system is already comparable to other similar commercial systems (Sorriento et al. 2020), further improvement could be achieved if a global volume calibration of the magnetic field model is performed. The motion platform introduced in Section 2.2 can be used to collect magnetic field data within the ROI, in order to improve the modelling step of Section 1.1.

Table 2 shows that the average solving time is almost 180% faster with C++ (18.4 ms for C++, versus 32.75 ms for Python) with a corresponding increase in the achievable update rates (54 Hz versus 30 Hz) compared to the Python implementation.

Comparison with the Matlab solver implementation is also included, although the significant memory overhead associated with this approach makes Matlab impractical in many real-life applications. It is also noted that the expected efficiency in memory allocation from C++ versus Python is significant, with an approximately 81% decrease (1.2 MB versus 97 MB) in memory for the solver implementation in C++.

The system performance in terms of accuracy and speed, reported in Table 1 and Table 2, meets the clinical requirements for a variety of surgical procedures, *e.g.*, pedicle screw insertion, tumor therapy, needles placement for percutaneous interventions, and thoracic–abdominal procedures (Yaniv et al. 2009; Lugez et al. 2015).

This work represents an important and logical step in the further development of open hardware for magnetic tracking. The results demonstrate the significant speed and efficiency benefits of a low-level C++ implementation, compared to previously reported approaches.

Future work should extend the implementation to use the C++ library as the back-end of a 3D Slicer module, thus allowing a user-friendly interface and fast and simple control of the various settings that can affect magnetic tracking accuracy.

The present results demonstrate the incentive to move to more open architectures for magnetic tracking, enabling low-level solver implementations in applications where high speed and precision are required, *e.g.*, in the next generation of robotic surgery devices.

5 References

Akhtar, Yusuf, Sarada Prasad Dakua, Alhusain Abdalla, Omar Mousa Aboumarzouk, Mohammed Yusuf Ansari, Julien Abinahed, Mohamed Soliman Mohamed Elakkad, and Abdulla Al-Ansari. 2021. 'Risk Assessment of Computer-Aided Diagnostic Software for Hepatic Resection'. *IEEE Transactions on Radiation and Plasma Medical Sciences*, 1–1. https://doi.org/10.1109/TRPMS.2021.3071148.

'Anser EMT | Open Science Framework'. n.d. Accessed 16 July 2021. https://osf.io/47q8q/.

Askeland, Christian, Ole Vegard Solberg, Janne Beate Lervik Bakeng, Ingerid Reinertsen, Geir Arne Tangen, Erlend Fagertun Hofstad, Daniel Høyer Iversen, et al. 2016. 'CustusX: An Open-Source Research Platform for Image-Guided Therapy'. *International Journal of Computer Assisted Radiology and Surgery* 11 (4): 505–19. https://doi.org/10.1007/s11548-015-1292-0.

Bien, Tomasz, Mengfei Li, Zein Salah, and Georg Rose. 2014. 'Electromagnetic Tracking System with Reduced Distortion Using Quadratic Excitation'. *International Journal of Computer Assisted Radiology and Surgery* 9 (2): 323–32. https://doi.org/10.1007/s11548-013-0925-4.

Brown, Alisa, Ali Uneri, Tharindu De Silva, Amir Manbachi, and Jeffrey H. Siewerdsen. 2018. 'Design and Validation of an Open-Source Library of Dynamic Reference Frames for Research and Education in Optical Tracking'. *Journal of Medical Imaging* 5 (2). https://doi.org/10.1117/1.JMI.5.2.021215.

Cavaliere, Marco, Herman Alexander Jaeger, Kilian O'Donoghue, and Pádraig Cantillon-Murphy. 2021. 'Planar Body-Mounted Sensors for Electromagnetic Tracking'. *Sensors* 21 (8): 2822. https://doi.org/10.3390/s21082822.

Cavaliere, Marco, Oisín McVeigh, H. Alexander Jaeger, Stephen Hinds, Kilian O'Donoghue, and Pádraig Cantillon-Murphy. 2020. 'Inductive Sensor Design for Electromagnetic Tracking in Image Guided Interventions'. *IEEE Sensors Journal*, 1–1. https://doi.org/10.1109/JSEN.2020.2984323.

Cleary, Kevin, and Terry M. Peters. 2010. 'Image-Guided Interventions: Technology Review and Clinical Applications'. *Annual Review of Biomedical Engineering* 12 (1): 119–42. https://doi.org/10.1146/annurev-bioeng-070909-105249.

De Angelis, Guido, Alessio De Angelis, Antonio Moschitta, and Paolo Carbone. 2017. 'Comparison of Measurement Models for 3D Magnetic Localization and Tracking'. *Sensors* 17 (11): 2527. https://doi.org/10.3390/s17112527.

'Electromagnetic Measurement Systems'. n.d. *NDI Europe GmbH* (blog). Accessed 24 August 2021. https://www.ndieurope.com/products/electromagnetic-products/.

Franz, Alfred Michael, Tamas Haidegger, Wolfgang Birkfellner, Kevin Cleary, Terry M. Peters, and Lena Maier-Hein. 2014. 'Electromagnetic Tracking in Medicine—A Review of Technology, Validation, and Applications'. *IEEE*

Transactions on Medical Imaging 33 (8): 1702–25. https://doi.org/10.1109/TMI.2014.2321777.

Franz, Alfred Michael, Herman Alexander Jaeger, Alexander Seitel, Pádraig Cantillon-Murphy, and Lena Maier-Hein. 2019. 'Open-Source Tracked Ultrasound with Anser Electromagnetic Tracking'. In *Bildverarbeitung für die Medizin 2019*, edited by Heinz Handels, Thomas M. Deserno, Andreas Maier, Klaus Hermann Maier-Hein, Christoph Palm, and Thomas Tolxdorff, 232–37. Informatik aktuell. Wiesbaden: Springer Fachmedien. https://doi.org/10.1007/978-3-658-25326-4_52.

Guennebaud, Gael, and Benoit Jacob. 2010. 'Eigen V3'. 2010. https://eigen.tuxfamily.org.

Halabi, Osama, Shidin Balakrishnan, Sarada Prasad Dakua, Nassir Navab, and Mohammed Warfa. 2020. 'Virtual and Augmented Reality in Surgery'. In *The Disruptive Fourth Industrial Revolution: Technology, Society and Beyond*, edited by Wesley Doorsamy, Babu Sena Paul, and Tshilidzi Marwala, 257–85. Lecture Notes in Electrical Engineering. Cham: Springer International Publishing. https://doi.org/10.1007/978-3-030-48230-5_11.

Haus, Hermann A, and James R Melcher. 1989. *Electromagnetic Fields and Energy*. Vol. 107. Prentice Hall Englewood Cliffs, NJ.

Jaeger, H. A., and P. Cantillon-Murphy. 2019. 'Electromagnetic Tracking Using Modular, Tiled Field Generators'. *IEEE Transactions on Instrumentation and Measurement* 68 (12): 4845–52. https://doi.org/10.1109/TIM.2019.2900884.

Jaeger, Herman Alexander, and Pádraig Cantillon-Murphy. 2018. 'Distorter Characterisation Using Mutual Inductance in Electromagnetic Tracking'. *Sensors* 18 (9): 3059. https://doi.org/10.3390/s18093059.

Jaeger, Herman Alexander, Alfred Michael Franz, Kilian O'Donoghue, Alexander Seitel, Fabian Trauzettel, Lena Maier-Hein, and Pádraig Cantillon-Murphy. 2017. 'Anser EMT: The First Open-Source Electromagnetic Tracking Platform for Image-Guided Interventions'. *International Journal of Computer Assisted Radiology and Surgery*. https://doi.org/10.1007/s11548-017-1568-7.

Jaeger, Herman Alexander, Stephen Hinds, and Pádraig Cantillon-Murphy. 2018. 'An Open Framework Enabling Electromagnetic Tracking in Image-Guided Interventions'. In *Lecture Notes in Computer Science (Including Subseries Lecture Notes in Artificial Intelligence and Lecture Notes in Bioinformatics)*, 11073 LNCS:168–75. https://doi.org/10.1007/978-3-030-00937-3_20.

Jaeger, Herman Alexander, Fabian Trauzettel, Pietro Nardelli, Federico Daverieux, Erlend Fagertun Hofstad, Håkon O. Leira, Marcus P. Kennedy, Thomas Langø, and Pádraig Cantillon-Murphy. 2019. 'Peripheral Tumour Targeting Using Open-Source Virtual Bronchoscopy with Electromagnetic Tracking: A Multi-User Pre-Clinical Study'. *Minimally Invasive Therapy & Allied Technologies* 28 (6): 363–72. https://doi.org/10.1080/13645706.2018.1544911.

Kikinis, Ron, Steve D. Pieper, and Kirby G. Vosburgh. 2014. '3D Slicer: A Platform for Subject-Specific Image Analysis, Visualization, and Clinical Support'. In *Intraoperative Imaging and Image-Guided Therapy*, edited by Ferenc A. Jolesz, 277–89. New York, NY: Springer. https://doi.org/10.1007/978-1-4614-7657-3_19.

Lee, Min Woo. 2014. 'Fusion Imaging of Real-Time Ultrasonography with CT or MRI for Hepatic Intervention'. *Ultrasonography* 33 (4): 227–39. https://doi.org/10.14366/usg.14021.

Levenberg, Kenneth. 1944. 'A Method for the Solution of Certain Non-Linear Problems in Least Squares'. *Quarterly of Applied Mathematics* 2 (2): 164–68. https://doi.org/10.1090/qam/10666.

Lugez, Elodie, Hossein Sadjadi, David R. Pichora, Randy E. Ellis, Selim G. Akl, and Gabor Fichtinger. 2015. 'Electromagnetic Tracking in Surgical and Interventional Environments: Usability Study'. *International Journal of Computer Assisted Radiology and Surgery* 10 (3): 253–62. https://doi.org/10.1007/s11548-014-1110-0.

Mansfield, Hilary, Padraig Cantillon-Murphy, James Griffiths, David Eustace, Michael O'Shea, Kilian O'Donoghue, and Timothy Power. 2014. 'Catheter Position Tracking System Using Planar Magnetics and Closed Loop Current Control'. *IEEE Transactions on Magnetics* 50 (7): 1–9. https://doi.org/10.1109/tmag.2014.2304271.

Peters, Terry, and Kevin Cleary, eds. 2008. *Image-Guided Interventions: Technology and Applications*. New York, NY: Springer Science+Business Media.

Plotkin, Anton, Oren Shafrir, Eugene Paperno, and Daniel M. Kaplan. 2010. 'Magnetic Eye Tracking: A New Approach Employing a Planar Transmitter'. *IEEE Transactions on Biomedical Engineering* 57 (5): 1209–15. https://doi.org/10.1109/TBME.2009.2038495.

Schwein, Adeline, Ben Kramer, Ponraj Chinnadurai, Sean Walker, Marcia O'Malley, Alan Lumsden, and Jean Bismuth. 2017. 'Flexible Robotics with Electromagnetic Tracking Improves Safety and Efficiency during in Vitro Endovascular Navigation'. *Journal of Vascular Surgery* 65 (2): 530–37. https://doi.org/10.1016/j.jvs.2016.01.045.

Schwein, Adeline, Benjamin Kramer, Ponraj Chinnadurai, Neha Virmani, Sean Walker, Marcia O'Malley, Alan B. Lumsden, and Jean Bismuth. 2018. 'Electromagnetic Tracking of Flexible Robotic Catheters Enables "Assisted Navigation" and Brings Automation to Endovascular Navigation in an in Vitro Study'. *Journal of Vascular Surgery* 67 (4): 1274–81. https://doi.org/10.1016/j.jvs.2017.01.072.

Shafrir, Oren, Eugene Paperno, and Anton Plotkin. 2010. *Magnetic Tracking with a Flat Transmitter*. LAP LAMBERT Academic Publishing. https://www.morebooks.shop/store/gb/book/magnetic-tracking-with-a-flat-transmitter/isbn/978-3-8383-4436-2.

Sonntag, C L W, M Sprée, E A Lomonova, J L Duarte, and A J A Vandenput. 2007. 'Accurate Magnetic Field Intensity Calculations for Contactless Energy Transfer Coils'. *Proceedings of the 16th International Conference on the Computation of Electromagnetic Fields, Achen, Germany*, 1–4.

Sorriento, Angela, Maria Bianca Porfido, Stefano Mazzoleni, Giuseppe Calvosa, Miria Tenucci, Gastone Ciuti, and Paolo Dario. 2020. 'Optical and Electromagnetic Tracking Systems for Biomedical Applications: A Critical Review on Potentialities and Limitations'. *IEEE Reviews in Biomedical Engineering* 13: 212–32. https://doi.org/10.1109/RBME.2019.2939091.

Tokuda, Junichi, Gregory S. Fischer, Xenophon Papademetris, Ziv Yaniv, Luis Ibanez, Patrick Cheng, Haiying Liu, et al. 2009. 'OpenIGTLink: An Open Network Protocol for Image-Guided Therapy Environment'. *International Journal of Medical Robotics and Computer Assisted Surgery* 5 (4): 423–34. https://doi.org/10.1002/rcs.274.

Ungi, Tamas, Andras Lasso, and Gabor Fichtinger. 2016. 'Open-Source Platforms for Navigated Image-Guided Interventions'. *Medical Image Analysis*, 20th anniversary of the Medical Image Analysis journal (MedIA), 33 (October): 181–86. https://doi.org/10.1016/j.media.2016.06.011.

Van Rossum, Guido, and Fred L. Drake. 2009. *Python 3 Reference Manual*. Scotts Valley, CA: CreateSpace.

Wilson, Emmanuel, Ziv Yaniv, David Lindisch, and Kevin Cleary. 2008. 'A Buyer's Guide to Electromagnetic Tracking Systems for Clinical Applications'. In *Medical Imaging 2008: Visualization, Image-Guided Procedures, and Modeling*, 6918:69182B. International Society for Optics and Photonics. https://doi.org/10.1117/12.770509.

Wolf, Ivo, Marcus Vetter, Ingmar Wegner, Marco Nolden, Thomas Böttger, Mark Hastenteufel, Max Schöbinger, Tobias Kunert, Hans-peter Meinzer, and Deutsches Krebsforschungszentrum. n.d. 'The Medical Imaging Interaction Toolkit (MITK) – a Toolkit Facilitating the Creation of Interactive Software by Extending VTK and ITK'.

Yaniv, Ziv, Emmanuel Wilson, David Lindisch, and Kevin Cleary. 2009. 'Electromagnetic Tracking in the Clinical Environment: Electromagnetic Tracking in the Clinical Environment'. *Medical Physics* 36 (3): 876–92. https://doi.org/10.1118/1.3075829.